Science and Technology Indonesia
e-ISSN:2580-4391 *p*-ISSN:2580-4405
Vol. 8, No. 4, October 2023

Research Paper

Fabrication and Characterization Fe_3O_4/Humic Acid for the Efficient Removal of Malachite Green

Nur Ahmad[1,2], Zaqiya Artha Zahara[2], Alfan Wijaya[2], Fitri Suryani Arsyad[3], Idha Royani[3], Aldes Lesbani[1,3]*

[1]*Doctoral Program of Natural Science, Graduate School Faculty of Mathematics and Natural Sciences, Universitas Sriwijaya, Sumatera Selatan, 30139, Indonesia*
[2]*Research Center Inorganic Center of Inorganic Materials and Complexes, Universitas Sriwijaya, Sumatera Selatan, 30139, Indonesia*
[3]*Master Program of Material Science, Graduate School Universitas Sriwijaya, Sumatera Selatan, 30139, Indonesia*
***Corresponding author**: aldeslesbani@pps.unsri.ac.id

Abstract
The dye pollutants that contaminate water and food resulting from commercial manufacture and illicit addiction are a worldwide threat that harms the ecosystem, the food supply, and the health of humans. Magnetite/Fe_3O_4 humic acid (MHA) with various ratios was synthesized using a two-step process involving coprecipitation and hydrothermal treatment in order to effectively overcome these obstacles. Analyses of SEM, XRD, FTIR, and VSM were used to describe the morphology and physicochemical aspects of MHA. The adsorption kinetics studies indicated that the adsorption mechanism of malachite green adhered to the pseudo-second-model and that the adsorption was adequately described by the Langmuir isotherm. The thermodynamic studies demonstrated spontaneous, endothermic, disorderly adsorption. MHA2 had maximal malachite green adsorption capacities of 83.333 mg/g. Malachite green and MHA may interact via π-π interaction, electrostatic attraction, van der Waals forces, H-bonding, pore filling, pore locking, and/or mechanical adhesion; however, physisorption dominates the adsorption process. Malachite green's adsorption characteristics change significantly after up to four cycles. It has been demonstrated that MHA has a high capacity for dye adsorption and a broad range of potential applications.

Keywords
Adsorption, Characterization, Humic Acid, Magnetite, Malachite Green

Received: 11 May 2023, Accepted: 13 August 2023
https://doi.org/10.26554/sti.2023.8.4.616-625

1. INTRODUCTION

Textile wastewater poses a significant environmental challenge as it leads to water pollution, which is essential for human survival (Dahlan et al., 2023; Gong et al., 2021; Santosa et al., 2021). In the industrial sector, approximately 100,000 dyes are utilized, resulting in the generation of textile wastewater (Fagbohun et al., 2022; Gao et al., 2022). Sadly, only 8% of this effluent gets processed instead of being released into waterways (Van Tran et al., 2022). This untreated wastewater poses a threat to the environment and human well-being due to the carcinogenic properties of these dyes (Ben et al., 2023). Malachite green (MG), one of the problematic dyes, is widely used in the fabrics, paper, and agricultural sectors (Brahma et al., 2022). MG has been linked to immune and reproductive system disruptions, as well as kidney failure (Kavci, 2021). Various technologies exist for removing dyes from textile wastewater, including degradation under visible light (Jabeen et al., 2023), membrane (Raval et al., 2022), biodegradation (Cheng et al., 2021), chemical oxidation (Al-Balawi et al., 2023), and adsorption (Rahman et al., 2021). The adsorption process is particularly advantageous due to its simplicity, effectiveness, efficiency, and cost-effectiveness (Palapa et al., 2023; Thotagamuge et al., 2021; Wu et al., 2022). Several adsorbents, such as halloysite nanotube (Altun and Ecevit, 2022), chitosan-zinc oxide (Muinde et al., 2020), ZnAl layered double hydroxide (Cardinale et al., 2022), and Fe-Zn nanoparticles (Gautam et al., 2015) have been reported as effective means of addressing this issue.

Humic acid (HA) is containing functional groups such as -COOH and -OH (Wang et al., 2023a; Zhao et al., 2023). It is a naturally occurring component found in soil organic matter, specifically belonging to the group of humic compounds (Sun et al., 2023b). HA possesses a notable adsorption capacity and is commonly utilized to adsorb both organic and inorganic pollutants (Zhang et al., 2023). Unfortunately, humic acid is susceptible to damage and presents challenges when separating it from aqueous solutions.

Magnetite (Fe_3O_4) is an iron oxide that falls under the mineral group known as spinel. It finds applications in various

fields such as water treatment, catalysts, membrane processes, and biodegradation through the process of adsorption (Paz et al., 2022; Wijaya and Yuliasari, 2023; Zong et al., 2022). The incorporation of magnetite imparts magnetic properties to HA, facilitating the separation of the adsorbent using an another magnet. Previous studies have reported the use of magnetite mixture to humic acid (MHA) for oxytetracycline adsorption, phosphate adsorption, and removal of pharmaceuticals (Lee and Kim, 2022; Tang et al., 2023; Yan et al., 2020).

The primary of this work is to prepare magnetite humic acid with different ratios through a combination of the conventional coprecipitation method and the subsequent hydrothermal process. The success of the synthesis was verified through the utilization of characterization techniques such as SEM, XRD, FTIR, and VSM analysis. The research also delved into multiple facets of adsorption, including an examination of kinetics, thermodynamics, and isotherms involved. Furthermore, regeneration techniques were used to determine the the durability of the MHA.

2. EXPERIMENTAL SECTION

2.1 Chemicals

The Humic Acid (HA) present in peat soil was sourced from the region of South Sumatra, Indonesia. The reagents used in this study, which comprised $FeCl_3$, $FeSO_4.7H_2O$, HCl, NaOH, and NH_3, were obtained from suppliers such as Merck and Sigma-Aldrich with analytical grade, without any further purification. Brataco provided the distilled water necessary for the experimental procedures.

2.2 Adsorbent Preparation

Magnetite/Fe_3O_4 humic acid (MHA) with different variation ratios was synthesized using a two-step process involving coprecipitation and hydrothermal treatment (Ahmad et al., 2023b). To initiate the synthesis, a mixture of $FeCl_3$ and $FeSO_4.7H_2O$ (ratio mol 3:1) was dissolved in 18 mL of distilled water through stirring. Subsequently, 3 g of humic acid (HA) was added to the solution and stirred for 3 h at room temperature. Next, NH_3 was slowly added to the mixture, followed by additional stirring for a half of hour at $75°C$. The resulting slurry was transferred to hydrothermal equipment, which lasted for 4 h at a temperature of $150°C$. After the hydrothermal process, the slurry was rinsed and dried at $100°C$. The resulting product obtained was Fe_3O_4/humic acid, specifically referred to as MHA3, indicating the 3:1 ratio of $FeCl_3$ and $FeSO_4.7H_2O$ used in its synthesis. Similarly, MHA2 and MHA1 were synthesized using the same procedures but with different ratios of $FeCl_3$ and $FeSO_4.7H_2O$, specifically 2:1 and 1.5:1, respectively.

2.3 Characterization

The morphological characteristics of MHA1, MHA2, and MHA3 were examined using a Scanning Electron Microscope (SEM) with a magnification of 1000 times, specifically the FEI Quanta 650 model. The crystalline structure of the adsorbents was analyzed using an X-Ray Diffractometer (XRD), specifically the Rigaku Miniflex-6000, with a scanning angle range of 10° to 70°. To assess the absorbance of malachite green, a UV-Visible Spectrophotometer (EMC) was employed, with a specific wavelength of 617 nm. The functional groups and magnetization properties of the adsorbent were characterized using Fourier Transfer Infra-Red (FTIR) spectroscopy, utilizing the Shimadzu Prestige-21 instrument within the wavenumber range of 500 cm^{-1} to 4000 cm^{-1} and the Vibrating Sample Magnetometer (VSM) VSM1.2H was utilized to measure the magnetic field within the range of -1 kOe to 1 kOe.

2.4 Adsorption Experiments

The concentration of a standard solution of malachite green (MG) was initially diluted to a concentration of 50 mg/L. Batch adsorption experiments were conducted to investigate the influence of various factors, including pHpzc (point of zero charges), temperature, contact time, and initial dye concentration. In each experimental run, 20 mL of the MG solution was mixed with 0.02 g of the adsorbent in a glass beaker, and the pHpzc has adjusted accordingly. The mixture was then subjected to agitation using a shaker. Subsequently, the final concentration of MG after adsorption was measured using a UV-Vis spectrophotometer at a wavelength of 617 nm. The adsorption capacity, denoted as the quantity adsorbed per unit mass of adsorbent (Q_t), was determined using the following Equation 1:

$$Q_t = \frac{(C_0 - C_t) \times V}{m} \quad (1)$$

Where C_0 represents the initial concentration of the MG (measured in mg/L); C_t corresponds to the concentration of the MG at any given time during the experiment (measured in mg/L); V signifies the volume of the MG solution (measured in L); lastly, m denoted the mass of the MHA1, MHA2, and MHA3 (measured in g).

3. RESULTS AND DISCUSSION

Morphology and chemical elements of MHA1, MHA2, and MHA3 are shown in Figure 1. Magnetite humic acid has irregular particles shapes, which means that the magnetite particles coated with humic acid do not have a consistent or uniform shape. The irregular particle shape observed in MHA is a result of various factors involved in the prepare material process and the interactions between the magnetite particles and the humic acid coating. It's worth noting that irregular particle shapes do not necessarily affect the performance of magnetite humic acid composites. Irregular shapes can sometimes enhance certain properties or interactions, such as increased surface area or improved adsorption capabilities (Zhou et al., 2014). The irregular shape can provide more active sites for adsorption. Meanwhile, the chemical elements of MHA1, MHA2, and MHA3 show that the Fe element increase with increasing ratio

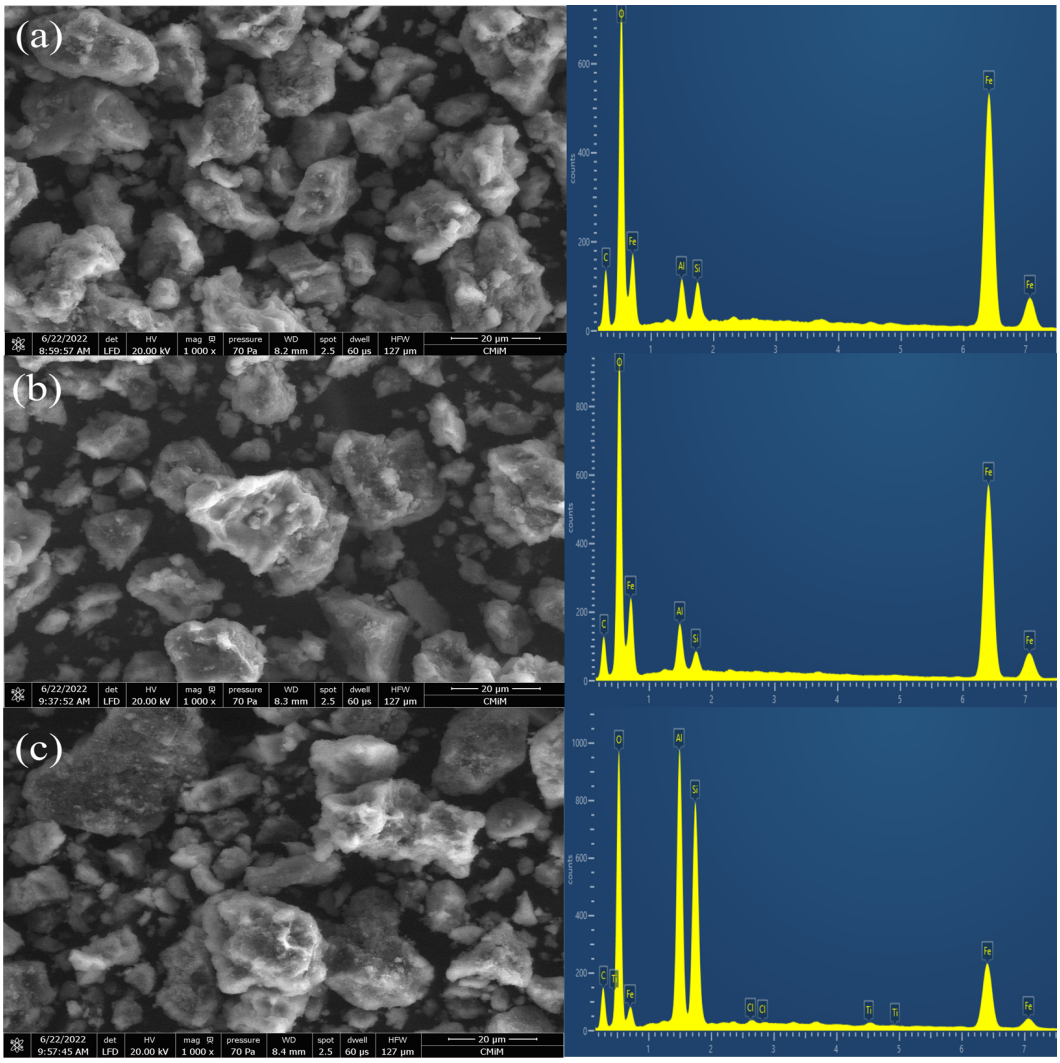

Figure 1. SEM-EDX Image of MHA3 (a), MHA2 (b), MHA1 (c)

of magnetite. So, MHA3 have Fe element higher than MHA1 and MHA2.

X-ray diffraction is a technique that provides valuable information about various aspects of crystalline materials, including their chemical composition, crystallographic structure, phase identification, and unit cell dimensions (Fan et al., 2023). In Figure 2, the powder X-ray diffraction pattern of MHA1, MHA2, and MHA3 is presented. The pattern exhibits prominent peaks at specific 2θ angles, namely 25.64°, 35.43°, and 62.91°. These peaks indicate the respective crystallographic planes (002), (311), and (440). The measured 2θ angles for magnetite samples are in good accordance with the values described on cards 19-0629 of the JCPDS, which functions as a reference for known crystallographic data (Prilepskii et al., 2018). The crystallographic planes of (002) have a 2θ peak shift because of changes in the chemical composition (magnetite ratio) of the crystal sample.

By measuring the bands of absorption, Fourier transforms infrared (FTIR) spectroscopy can learn useful details about the many functional groups. The presence of functional groups of MHA1, MHA2, and MHA3 was confirmed by FTIR results in Figure 3. The bands lower than 1000 cm^{-1} (541, 795, and 909 cm^{-1}) were due to metal-oxygen bonds (Fe-O and Fe-O-Fe) (Amin et al., 2023; Kotnala et al., 2023; Li et al., 2021). The presence of peaks at 1026 and 1395 cm^{-1} was attributed to the stretching of C-O-C and bending of $HCOO^-$ on humic acid (Wang, Huang, Sheng, and Ma, 2023b). Two bands at 1603 and 3424 cm^{-1} were confirmed aromatic rings of the C-C group and OH stretching vibrations (Khan and Bagla, 2022; Sun et al., 2023a).

Vibrating sample magnetometer (VSM) measures the strength of magnetization of MHA1, MHA2, and MHA3 as an effect of magnetic field and temperature. The hysteresis loops of the MHA1, MHA2, and MHA3 at room temperature are depicted in Figure 4. The S-shaped magnetic hysteresis loop of MHA1, MHA2, and MHA3 confirms the materials' super-

Table 1. Kinetic Fitting Parameters

Adsorbent	Q_{eexp} (mg/g)	PFO			PSO		
		Q_{ecalc} (mg/g)	k_1 (min^{-1})	R^2	Q_{ecalc} (mg/g)	k_2 (g/mg.min)	R^2
MHA1	41.526	16.342	0.023	0.887	42.553	0.004	0.999
MHA2	45.733	15.937	0.026	0.896	46.512	0.005	0.999
MHA3	39.03	13.041	0.019	0.957	40.161	0.003	0.999

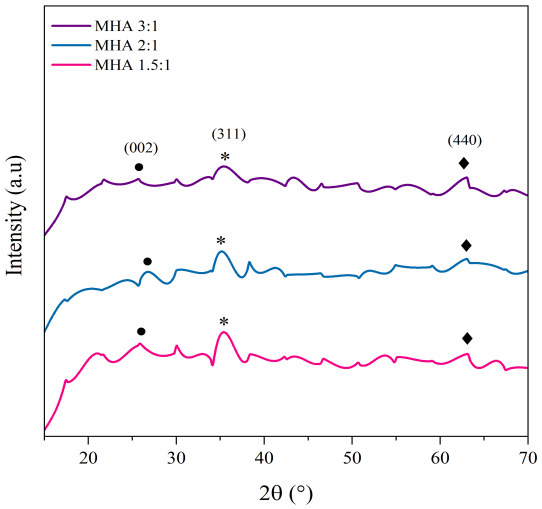

Figure 2. X-Ray Diffraction Pattern of MHA1, MHA2, and MHA3

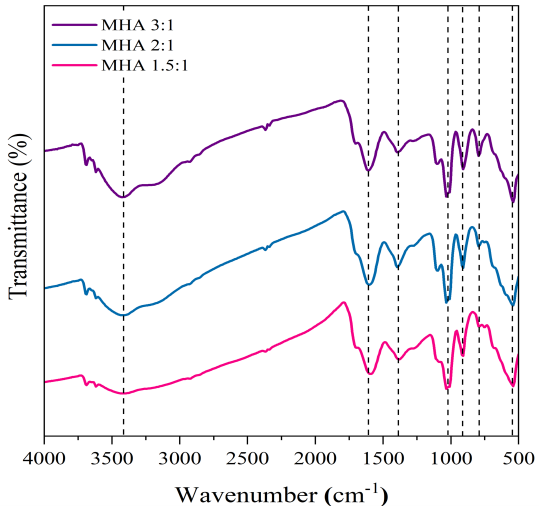

Figure 3. FTIR of MHA1, MHA2, and MHA3

paramagnetic behavior (Das and Dhar, 2020). MHA1, MHA2, and MHA3 exhibit strong magnetic behavior with saturation magnetization values of 13.829, 15.512, and 20.320 emu/g, respectively. As the material exhibits superparamagnetic properties, it can be easily extracted or gathered by another magnet (Li et al., 2023).

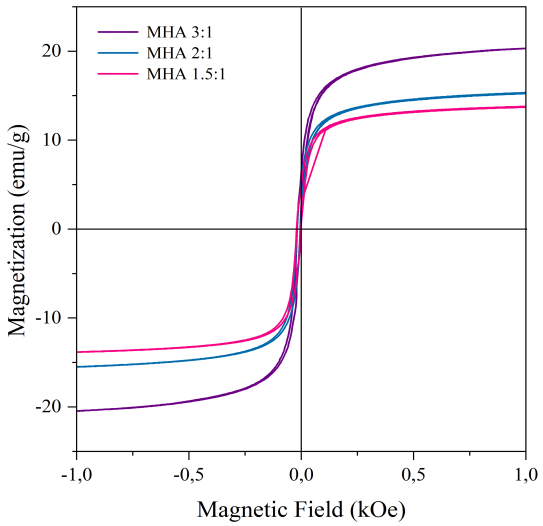

Figure 4. VSM Graphic

To analyze the adsorption kinetics, the pseudo-first-order (PFO) and pseudo-second-order (PSO) models were employed. The Equations 2 and 3 used for these models are as follows:

$$\log(Q_e - Q_t) = \log Q_e - \left(\frac{k_1}{2.303}\right) \times t \quad (2)$$

$$\frac{1}{Q_t} = \frac{1}{k_2 Q_t^2} + \frac{1}{Q_e} \quad (3)$$

In these equations, Q_e represents the adsorption capacity at equilibrium and Q_t represents the adsorption capacity at time t (both measured in mg/g); the rate constraints for the PFO and PSO models are denoted as k_1 (in min^{-1}) and k_2 (in g/mg.min), respectively; the variable t represents the adsorption time of MG (in min).

The experimental adsorption data were fitted with kinetics and isotherm models to obtain useful knowledge of the adsorption process and behavior (Siraorarnroj et al., 2022). The resulting fitting lines of both of the kinetics models are shown in Figure 5, and the associated variables are specified in Table 1. Based on the given information, it appears that the PSO model provides a better fit to experimental data, as indicated by the higher R^2 values compared to the PFO model. The calculated

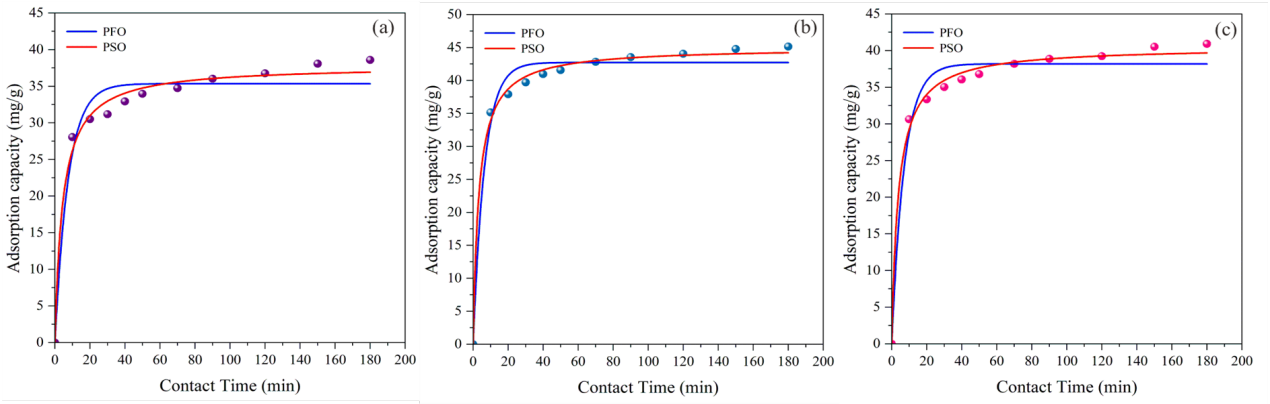

Figure 5. Kinetics Parameters of MHA3 (a), MHA2 (b), and MHA1 (c)

Table 2. Isotherm Fitting Parameters

Adsorbent	T (°C)	Langmuir			Freundlich		
		Q_{max} (mg/g)	K_L (mg/L)	R^2	n	K_F	R^2
MHA1	30	14.925	1.151	0.999	0.958	1.037	0.976
	40	28.571	0.312	0.998	0.933	1.129	0.945
	50	45.455	0.198	0.996	0.958	1.462	0.914
	60	35.714	0.475	0.999	1.130	2.985	0.956
MHA2	30	81.301	0.067	0.968	2.613	14.618	0.881
	40	83.333	0.085	0.988	2.799	17.807	0.921
	50	62.500	0.116	0.990	2.484	16.873	0.951
	60	71.429	0.123	0.993	2.597	19.333	0.959
MHA3	30	15.385	0.603	0.991	4.606	23.594	0.865
	40	19.608	0.544	0.990	4.621	26.080	0.890
	50	24.390	0.458	0.992	4.255	26.278	0.924
	60	55.556	0.271	0.994	4.617	30.040	0.915

Table 3. Comparison of Malachite Green Adsorption onto Several Adsorbents

Adsorbents	Q_{max} (mg/g)	Reference
PANI/CNT	15.45	(Zeng et al., 2013)
Fe_3O_4/ epoxy-triazinetrione	23.92	(Bakhshi Nejad and Mohammadi, 2020)
Chitosan/ZnO nanoparticles	11	(Muinde et al., 2020)
MWCNT-COOH	11.73	(Rajabi et al., 2016)
$CoFe_2O_4$@SiO_2	75.50	(Amiri et al., 2017)
Rice husk bio-char	67.6	(Leng et al., 2015)
Peach-AC	73.53	(Qu et al., 2019)
MHA1	45.455	This study
MHA2	83.333	This study
MHA3	55.556	This study

Q_e values using the PSO model also tend to be closer to the experimental values. The PSO indicated a chemical process and assumed that the rate of adsorption is dependent on the square of the amount of adsorbate on the surface (Hoang et al., 2020).

The equilibrium adsorption isotherms were analyzed using two models: the Langmuir and Freundlich isotherm models. These models can be described by Equations 4 and 5, respectively:

$$\frac{C_e}{Q_e} = \frac{C_e}{Q_{max}} + \frac{1}{Q_{max}K_L} \quad (4)$$

Table 4. Thermodynamics of Malachite Green Adsorption in 60 mg/L

Adsorbent	ΔH (kJ/mol)	ΔS (J/K.mol)	ΔG (kJ/mol) 30°C	40°C	50°C	60°C
MHA1	11.301	0.039	-0.455	-0.843	-1.231	-1.619
MHA2	14.389	0.055	-2.353	-2.905	-3.458	-4.010
MHA3	17.457	0.066	-2.436	-3.093	-3.749	-4.406

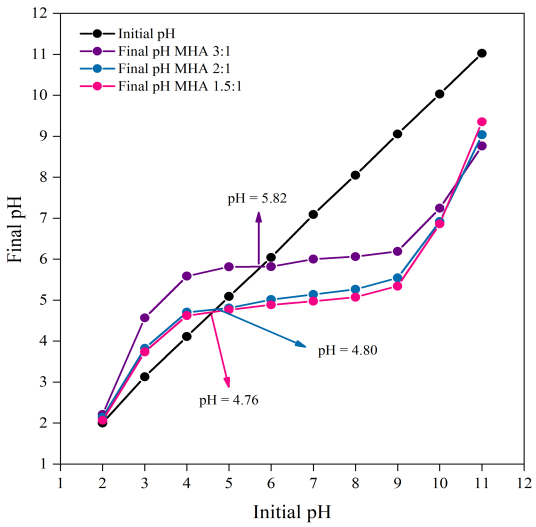

Figure 6. pHpzc of MHA1, MHA2, and MHA3

$$\log Q_e = \log K_F - \frac{1}{n} \log C_e \tag{5}$$

In the Langmuir model, C_e represents the equilibrium concentration of MG (measured in mg/L), while Q_e (measured in mg/g) represents the corresponding equilibrium adsorption capacity (mg/g); Q_{max} is the maximum adsorption capacity of the adsorbent (measured in mg/g); and K_L is the Langmuir constant (measured in L/mg). For the Freundlich model K_F is the Freundlich constant, representing the adsorption capacity, and n is the Freundlich exponent, indicating the favorability and intensity of adsorption. By fitting experimental data into these models, valuable insights into the adsorption behavior of MG onto adsorbents can be gained. Examining the isotherm is possibly helpful for determining the adsorption behavior and maximum capacity for adsorption of MHA1, MHA2, and MHA. The isotherm curves fit the Langmuir model with a higher R^2 value more closely, indicating that the malachite green adsorption processes belong to monolayer adsorption based on Table 2's results (Jin et al., 2022). Based on Langmuir isotherm, the Q_{max} values for MHA1, MHA2, and MHA3 are 45.455, 83.333, and 55.556 mg/g, respectively. Previous studies about the adsorption of malachite green are shown in Table 3.

The equilibrium adsorption process was investigated in terms of thermodynamics by employing two important equations: Equation 6 and 7. Equation 7 relates the natural logarithm of the ratio of the equilibrium adsorption capacity (Q_e) to the equilibrium concentration of malachite green (C_e) with the thermodynamic parameters:

$$\ln \frac{Q_e}{C_e} = \frac{\Delta S}{R} - \frac{\Delta H}{RT} \tag{6}$$

$$\Delta G^\circ = \Delta H - T\Delta S \tag{7}$$

where C_e is the concentration of malachite green at equilibrium (measured in mg/L); Q_e (mg/g) represents the corresponding adsorption capacity at equilibrium (measured in mg/g); ΔS denotes the entropy change associated with the adsorption process (measured in J/mol·K. ΔH represents the enthalpy change (measured in kJ/mol).; R is the ideal gas constant (measured in J/mol·K); T is the temperature of the system (measured in Kelvin). In Equation 7, ΔG° represents the standard Gibbs free energy change (measured in kJ/mol). These parameters provide a deeper understanding of the energetics and potential MHA to adsorption of malachite green.

The thermodynamic parameters are detailed in Table 4. According to the enthalpy values of 11.301, 14.389, and 17.457 kJ/mol, the adsorption of a malachite green molecule on MHA1, MHA2, and MHA3 occurs endothermic. Enthalpy's value is below 40 kJ/mol, indicating that the mechanism is physisorption between malachite green and the active site of MHA (Yönten et al., 2020). The positive value of ΔS suggests that structural changes in malachite green and MHA are caused by an increase in randomness at the solid-liquid (Sarkar et al., 2021). Negative Gibbs free energy (ΔG) demonstrates that the adsorption process occurs spontaneously. The increase of ΔG negativity with temperature suggests that "favorability" increases with temperature (Ahmed et al., 2021). Malachite green adsorption on MHA1, MHA2, and MHA3 occurs by physisorption, endothermic, and spontaneous.

The value of pH can influence the MHA1, MHA2, and MHA3 surface charge, the release of chemical groups on the active adsorbent sites, the ionization degree of chemical contaminants, and the composition of the dye (Grover et al., 2022). pHpzc of MHA1, MHA2, and MHA3 was obtained at pH 5.82, 4.80, and 4.76, respectively (Figure 6). When the solution pH is less than pHpzc, the positive charge on the MHA can be

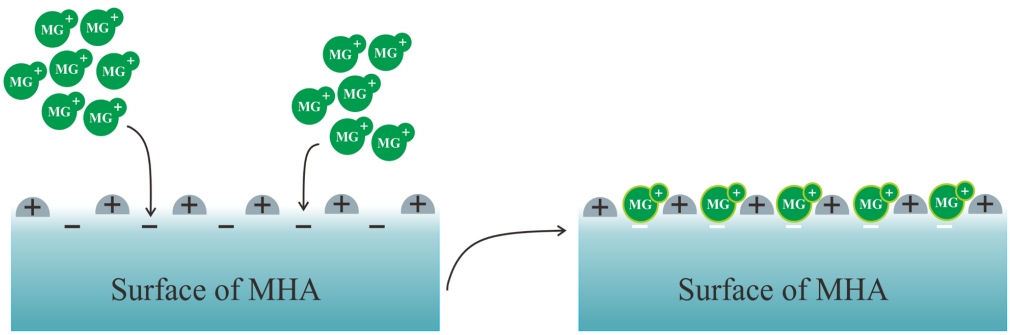

Figure 7. Proposed Adsorption Mechanism of Malachite Green onto MHA1, MHA2, and MHA3

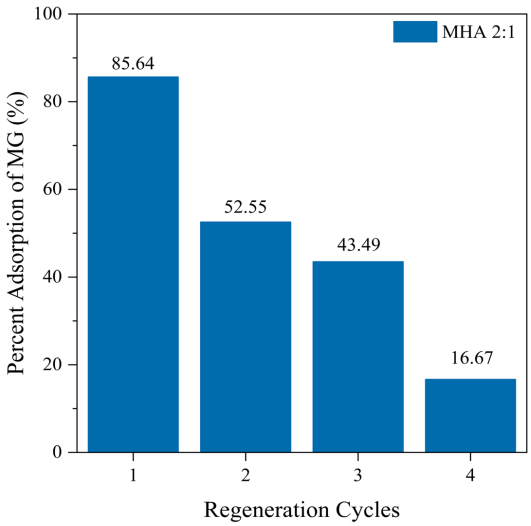

Figure 8. Regeneration Cycles of MHA2

predominate. Meanwhile, When the solution pH is greater than pHpzc, the negative charge dominates the MHA (Ahmad et al., 2023a). In this investigation, the malachite green adsorption process was conducted in pHpzc. Hope, the physisorption from the adsorbent can be maximal to remove the dye. Although malachite green and MHA may interact via π-π interaction, electrostatic attraction, van der Waals forces, H-bonding, pore filling, pore locking, and/or mechanical adhesion. Figure 7 illustrates the proposed mechanism of malachite green's adsorption onto MHA1, MHA2, and MHA3.

The regeneration of used adsorbents is an essential concern from an economic and environmental standpoint (Tang et al., 2023). After adsorption, the used MHA was washed with water and desorbed for 15 min using an ultrasonic device. This study tests this property using 50 mg/L of malachite green for MHA2. MHA2 was selected due to its high absorption capacity. Malachite green's adsorption characteristics change significantly after up to four cycles (Figure 8). The malachite green rejection efficiency could remain at 16.67%. This result revealed that MHA2 may have additional applications in the treatment of malachite green pollutants.

4. CONCLUSION

In this study, various ratios of magnetite humic acid (MHA) were synthesized for the adsorption of malachite green. Validation of the successful material of the components was conducted using SEM, XRD, FTIR, and VSM. The highest malachite green adsorption capacities for MHA2 were 83.333 mg/g. The highest adsorption capacity (Q_{max}) confirmed MHA's capacity to adsorb malachite green. Although electrostatic attraction, H-bonding, π-π interaction, van der Waals forces, pore filling, pore locking, and/or mechanical adhesion are possible interactions between malachite green and MHA, physisorption dominates the adsorption process. Malachite green and MHA may interact via π-π interaction, electrostatic attraction, van der Waals forces, H-bonding, pore filling, pore locking, and/or mechanical adhesion; however, physisorption dominates the adsorption process. From the reusability investigation, it can be concluded that MHA can be reused multiple times for the malachite green adsorption.

5. ACKNOWLEDGMENT

The authors gratefully appreciate the grant funding of the Kementerian Pendidikan, Kebudayaan, Riset, dan Teknologi, Indonesia with HIBAH PMDSU 2022-2024 according to agreement numbers 059/E5/PG.02.00.PL/2023 and 0195/UN9.3.1/PL/2023. Additionally, the author thanks the Research Center of Inorganic Materials and Complexes at Universitas Sriwijaya for analytical services and guidance.

REFERENCES

Ahmad, N., F. S. Arsyad, I. Royani, and A. Lesbani (2023a). Charcoal Activated as Template Mg/Al Layered Double Hydroxide for Selective Adsorption of Direct Yellow on Anionic Dyes. *Results in Chemistry*, **5**; 100766

Ahmad, N., F. S. Arsyad, I. Royani, P. M. S. B. N. Siregar, T. Taher, and A. Lesbani (2023b). High Regeneration of

ZnAl/NiAl-Magnetite Humic Acid for Adsorption of Congo Red from Aqueous Solution. *Inorganic Chemistry Communications*, **150**; 110517

Ahmed, S., H. U. Rehman, Z. Ali, A. Qadeer, A. Haseeb, and Z. Ajmal (2021). Solvent Assisted Synthesis of Hierarchical Magnesium Oxide Flowers for Adsorption of Phosphate and Methyl Orange: Kinetic, Isotherm, Thermodynamic and Removal Mechanism. *Surfaces and Interfaces*, **23**; 100953

Al-Balawi, A. M., Z. Zaheer, and S. A. Kosa (2023). Silver-Platinum Bimetallic Nanoparticles as Heterogeneous Persulfate Activator for the Oxidation of Malachite Green. *Arabian Journal of Chemistry*, **16**(8); 104863

Altun, T. and H. Ecevit (2022). Adsorption of Malachite Green and Methyl Violet 2B by Halloysite Nanotube: Batch Adsorption Experiments and Box-Behnken Experimental Design. *Materials Chemistry and Physics*, **291**; 126612

Amin, K. F., F. Gulshan, F. Asrafuzzaman, H. Das, R. Rashid, and S. M. Hoque (2023). Synthesis of Mesoporous Silica and Chitosan-Coated Magnetite Nanoparticles for Heavy Metal Adsorption from Wastewater. *Environmental Nanotechnology, Monitoring & Management*, **20**; 100801

Amiri, M., M. Salavati-Niasari, A. Akbari, and T. Gholami (2017). Removal of Malachite Green (a Toxic Dye) from Water by Cobalt Ferrite Silica Magnetic Nanocomposite: Herbal and Green Sol-Gel Autocombustion Synthesis. *International Journal of Hydrogen Energy*, **42**(39); 24846–24860

Bakhshi Nejad, S. and A. Mohammadi (2020). Epoxy-Triazinetrione-Functionalized Magnetic Nanoparticles as an Efficient Magnetic Nanoadsorbent for the Removal of Malachite Green and Pb (II) from Aqueous Solutions. *Journal of Chemical & Engineering Data*, **65**(5); 2731–2742

Ben, S. K., S. Gupta, K. K. Raj, and V. Chandra (2023). Adsorption of Malachite Green from Polyaniline Facilitated Cobalt Phosphate Nanocomposite from Aqueous Solution. *Chemical Physics Letters*, **820**; 140469

Brahma, D., H. Nath, D. Borah, M. Debnath, and H. Saikia (2022). Coconut Husk Ash Fabricated CoAl-Layered Double Hydroxide Composite for the Enhanced Sorption of Malachite Green Dye: Isotherm, Kinetics and Thermodynamic Studies. *Inorganic Chemistry Communications*; 109878

Cardinale, A. M., C. Carbone, M. Fortunato, B. Fabiano, and A. P. Reverberi (2022). ZnAl-SO_4 Layered Double Hydroxide and Allophane for Cr (VI), Cu (II) and Fe (III) Adsorption in Wastewater: Structure Comparison and Synergistic Effects. *Materials*, **15**(19); 6887

Cheng, C. M., A. K. Patel, R. R. Singhania, C. H. Tsai, S. Y. Chen, C. W. Chen, and C. Di Dong (2021). Heterologous Expression of Bacterial CoTa-Laccase, Characterization and Its Application for Biodegradation of Malachite Green. *Bioresource Technology*, **340**; 125708

Dahlan, I., O. H. Keat, H. A. Aziz, and Y. T. Hung (2023). Synthesis and Characterization of MOF-5 Incorporated Waste-Derived Siliceous Materials for the Removal of Malachite Green Dye from Aqueous Solution. *Sustainable Chemistry and Pharmacy*, **31**; 100954

Das, K. C. and S. S. Dhar (2020). Rapid Catalytic Degradation of Malachite Green by $MgFe_2O_4$ Nanoparticles in Presence of H_2O_2. *Journal of Alloys and Compounds*, **828**; 154462

Fagbohun, E. O., Q. Wang, L. Spessato, Y. Zheng, W. Li, A. G. Olatoye, and Y. Cui (2022). Physicochemical Regeneration of Industrial Spent Activated Carbons Using a Green Activating Agent and Their Adsorption for Methyl Orange. *Surfaces and Interfaces*, **29**; 101696

Fan, S., X. Fan, S. Wang, B. Li, N. Zhou, and H. Xu (2023). Effect of Chitosan Modification on the Properties of Magnetic Porous Biochar and Its Adsorption Performance Towards Tetracycline and Cu^{2+}. *Sustainable Chemistry and Pharmacy*, **33**; 101057

Gao, L., T. Gao, Y. Zhang, and T. Hu (2022). A Bifunctional 3D Porous Zn-MOF: Fluorescence Recognition of Fe^{3+} and Adsorption of Congo Red/methyl Orange Dyes in Aqueous Medium. *Dyes and Pigments*, **197**; 109945

Gautam, R. K., V. Rawat, S. Banerjee, M. A. Sanroman, S. Soni, S. K. Singh, and M. C. Chattopadhyaya (2015). Synthesis of Bimetallic Fe–Zn Nanoparticles and Its Application Towards Adsorptive Removal of Carcinogenic Dye Malachite Green and Congo Red in Water. *Journal of Molecular Liquids*, **212**; 227–236

Gong, L., H. Wu, X. Shan, and Z. Li (2021). Facile Fabrication of Phosphorylated Alkali Lignin Microparticles for Efficient Adsorption of Antibiotics and Heavy Metal Ions in Water. *Journal of Environmental Chemical Engineering*, **9**(6); 106574

Grover, A., I. Mohiuddin, J. Lee, R. J. Brown, A. K. Malik, J. S. Aulakh, and K. H. Kim (2022). Progress in Pre-Treatment and Extraction of Organic and Inorganic Pollutants by Layered Double Hydroxide for Trace-Level Analysis. *Environmental Research*; 114166

Hoang, L. P., H. T. Van, T. T. H. Nguyen, V. Q. Nguyen, and P. Quang Thang (2020). Coconut Shell Activated Carbon/$CoFe_2O_4$ Composite for the Removal of Rhodamine B from Aqueous Solution. *Journal of Chemistry*, **2020**; 1–12

Jabeen, S., A. S. Ganie, N. Ahmad, S. Hijazi, S. Bala, D. Bano, and T. Khan (2023). Fabrication and Studies of $LaFe_2O_3/Sb_2O_3$ Heterojunction for Enhanced Degradation of Malachite Green Dye under Visible Light Irradiation. *Inorganic Chemistry Communications*, **152**; 110729

Jin, C., Y. Liu, J. Fan, T. Liu, G. Liu, F. Chu, and Z. Kong (2022). Lignin-Inspired Porous Polymer Networks as High-Performance Adsorbents for the Efficient Removal of Malachite Green Dye. *Colloids and Surfaces A: Physicochemical and Engineering Aspects*, **643**; 128760

Kavci, E. (2021). Malachite Green Adsorption onto Modified Pine Cone: Isotherms, Kinetics and Thermodynamics Mechanism. *Chemical Engineering Communications*, **208**(3); 318–327

Khan, A. N. and H. K. Bagla (2022). Batch Adsorption and Desorption Investigations of Cs (I) and Sr (II) from Simulated Reactor Waste by Humic Acid. *Journal of Trace Elements and Minerals*, **1**; 100005

Kotnala, S., B. Bhushan, and A. Nayak (2023). Fabrication of a

Magnetite Hydroxyapatite Nanocomposite for the Removal of Paraquat Dichloride: Adsorption Studies. *Materials Today: Proceedings*, **73**; 122–127

Lee, W. H. and J. O. Kim (2022). Phosphate Recovery from Anaerobic Digestion Effluent Using Synthetic Magnetite Particles. *Journal of Environmental Chemical Engineering*, **10**(1); 107103

Leng, L., X. Yuan, G. Zeng, J. Shao, X. Chen, Z. Wu, H. Wang, and X. Peng (2015). Surface Characterization of Rice Husk Bio-Char Produced by Liquefaction and Application for Cationic Dye (malachite Green) Adsorption. *Fuel*, **155**; 77–85

Li, D., T. Hua, J. Yuan, and F. Xu (2021). Methylene Blue Adsorption from an Aqueous Solution by a Magnetic Graphene Oxide/humic Acid Composite. *Colloids and Surfaces A: Physicochemical and Engineering Aspects*, **627**; 127171

Li, H., Z. Yuan, S. Ding, and J. Yuan (2023). Adsorption of Lead Ions by Magnetic Carbon: Comparison of Magnetic Carbon Properties and Modification Methods. *Journal of Environmental Chemical Engineering*, **11**(3); 110136

Muinde, V. M., J. M. Onyari, B. Wamalwa, and J. N. Wabomba (2020). Adsorption of Malachite Green Dye from Aqueous Solutions Using Mesoporous Chitosan–Zinc Oxide Composite Material. *Environmental Chemistry and Ecotoxicology*, **2**; 115–125

Palapa, N., N. Ahmad, A. Wijaya, and Z. Zahara (2023). Facile Fabrication of Layered Double Hydroxide-Lignin for Efficient Adsorption of Malachite Green. *Science and Technology Indonesia*, **8**; 305–311

Paz, M. J., T. Vieira, H. Enzweiler, and A. T. Paulino (2022). Chitosan/wood Sawdust/magnetite Composite Membranes for the Photodegradation of Agrochemicals in Water. *Journal of Environmental Chemical Engineering*, **10**(1); 106967

Prilepskii, A. Y., A. F. Fakhardo, A. S. Drozdov, V. V. Vinogradov, I. P. Dudanov, A. A. Shtil, P. P. Bel'tyukov, A. M. Shibeko, E. M. Koltsova, D. Y. Nechipurenko, and V. V. Vinogradov (2018). Urokinase-Conjugated Magnetite Nanoparticles as a Promising Drug Delivery System for Targeted Thrombolysis: Synthesis and Preclinical Evaluation. *ACS applied materials & interfaces*, **10**(43); 36764–36775

Qu, W., T. Yuan, G. Yin, S. Xu, Q. Zhang, and H. Su (2019). Effect of Properties of Activated Carbon on Malachite Green Adsorption. *Fuel*, **249**; 45–53

Rahman, M. T., T. Kameda, T. Miura, S. Kumagai, and T. Yoshioka (2021). Removal of Sulfate from Wastewater via Synthetic Mg–Al Layered Double Hydroxide: An Adsorption, Kinetics, and Thermodynamic Study. *Journal of the Indian Chemical Society*, **98**(11); 100185

Rajabi, M., B. Mirza, K. Mahanpoor, M. Mirjalili, F. Najafi, O. Moradi, H. Sadegh, R. Shahryari-Ghoshekandi, M. Asif, I. Tyagi, S. Agarwal, and V. K. Gupta (2016). Adsorption of Malachite Green from Aqueous Solution by Carboxylate Group Functionalized Multi-Walled Carbon Nanotubes: Determination of Equilibrium and Kinetics Parameters. *Journal of Industrial and Engineering Chemistry*, **34**; 130–138

Raval, A. R., H. P. Kohli, and O. K. Mahadwad (2022). Application of Emulsion Liquid Membrane for Removal of Malachite Green Dye from Aqueous Solution: Extraction and Stability Studies. *Chemical Engineering Journal Advances*, **12**; 100398

Santosa, S. J., P. A. Krisbiantoro, T. T. M. Ha, N. T. T. Phuong, and G. Gusrizal (2021). Composite of Magnetite and Zn/Al Layered Double Hydroxide as a Magnetically Separable Adsorbent for Effective Removal of Humic Acid. *Colloids and Surfaces A: Physicochemical and Engineering Aspects*, **614**; 126159

Sarkar, S., N. Tiwari, A. Basu, M. Behera, B. Das, S. Chakrabortty, K. Sanjay, M. Suar, T. K. Adhya, S. Banerjee, and S. K. Tripathy (2021). Sorptive Removal of Malachite Green from Aqueous Solution by Magnetite/coir Pith Supported Sodium Alginate Beads: Kinetics, Isotherms, Thermodynamics and Parametric Optimization. *Environmental Technology & Innovation*, **24**; 101818

Siraorarnroj, S., N. Kaewtrakulchai, M. Fuji, and A. Eiad-ua (2022). High Performance Nanoporous Carbon from Mulberry leaves *(Morus alba* L.) Residues via Microwave Treatment Assisted Hydrothermal-Carbonization for Methyl Orange Adsorption: Kinetic, Equilibrium and Thermodynamic Studies. *Materialia*, **21**; 101288

Sun, N., J. Liu, B. W. Qi, L. L. Lu, H. L. Du, S. Li, C. Q. Li, S. W. Jiang, Z. J. Wang, A. P. Yang, G. L. Z. Zhu, T. Y. Wang, S. M. Wang, and Q. Fu (2023a). Effect of Humic Acid-Modified Attapulgite on Polycyclic Aromatic Hydrocarbon Adsorption and Release from Paddy Soil into the Overlying Water in a Rice-Crab Coculture Paddy Ecosystem and the Underlying Process. *Chemosphere*, **329**; 138555

Sun, Q., H. Zhou, C. Xu, Y. Ba, Z. Geng, and D. She (2023b). Effective Adsorption of Ammonium Nitrogen by Sulfonic-Humic Acid Char and Assessment of Its Recovery for Application as Nitrogen Fertilizer. *Science of The Total Environment*, **867**; 161591

Tang, Y., X. Zhang, X. Li, J. Bai, C. Yang, Y. Zhang, Z. Xu, X. Jin, and Y. Jiang (2023). Facile Synthesis of Magnetic ZnAl Layered Double Hydroxides and Efficient Adsorption of Malachite Green and Congo Red. *Separation and Purification Technology*; 124305

Thotagamuge, R., M. R. R. Kooh, A. H. Mahadi, C. M. Lim, M. Abu, A. Jan, A. H. A. Hanipah, Y. Y. Khiong, and A. Shofry (2021). Copper Modified Activated Bamboo Charcoal to Enhance Adsorption of Heavy Metals from Industrial Wastewater. *Environmental Nanotechnology, Monitoring & Management*, **16**; 100562

Van Tran, T., D. T. C. Nguyen, P. S. Kumar, A. T. M. Din, A. S. Qazaq, and D. V. N. Vo (2022). Green Synthesis of Mn_3O_4 Nanoparticles Using *Costus woodsonii* Flowers Extract for Effective Removal of Malachite Green Dye. *Environmental research*, **214**; 113925

Wang, Q., Y. Zhang, H. Chen, S. Chen, and Y. Wang (2023a). Effects of Humic Acids on the Adsorption of Pb (II) Ions onto Biofilm-Developed Microplastics in Aqueous Ecosys-

tems. *Science of The Total Environment*, **882**; 163466

Wang, Y., Z. Huang, L. Sheng, and Y. Ma (2023b). Effect of Modified Humic Acid Residue on the Adsorption and Passivation of Hg^{2+}/Pb^{2+} in Solution and Soil. *Journal of Molecular Liquids*, **377**; 121581

Wijaya, A. and N. Yuliasari (2023). Biochar Derived from Rice Husk as Effective Adsorbent for the Removal Congo Red and Procion Red MX-5B Dyes. *Indonesian Journal of Material Research*, **1**(1); 1–7

Wu, F., L. Chen, P. Hu, X. Zhou, H. Zhou, D. Wang, X. Lu, and B. Mi (2022). Comparison of Properties, Adsorption Performance and Mechanisms to Cd (II) on Lignin-Derived Biochars under Different Pyrolysis Temperatures by Microwave Heating. *Environmental Technology & Innovation*, **25**; 102196

Yan, C., L. Fan, Y. Chen, and Y. Xiong (2020). Effective Adsorption of Oxytetracycline from Aqueous Solution by Lanthanum Modified Magnetic Humic Acid. *Colloids and Surfaces A: Physicochemical and Engineering Aspects*, **602**; 125135

Yönten, V., N. Karaca Sanyürek, and M. Kıvanç (2020). A Thermodynamic and Kinetic Approach to Adsorption of Methyl Orange from Aqueous Solution Using a Low Cost Activated Carbon Prepared from *Vitis vinifera* L. *Surfaces and Interfaces*, **20**; 100529

Zeng, Y., L. Zhao, W. Wu, L. Guixia, F. Xu, Y. Tong, W. Liu, and J. Du (2013). Enhanced Adsorption of Malachite Green onto Carbon Nanotube/polyaniline Composites. *Journal of Applied Polymer Science*, **127**

Zhang, J., X. Li, H. Xu, W. Zhang, X. Feng, Y. Yao, Y. Ma, L. Su, S. Ren, and S. Li (2023). Removal of Cd^{2+}, Pb^{2+} and Ni^{2+} from Water by Adsorption onto Magnetic Composites Prepared Using Humic Acid from Waste Biomass. *Journal of Cleaner Production*, **411**; 137237

Zhao, P., Z. Huang, P. Wang, Z. Fu, A. Wang, and L. Sheng (2023). Two Recyclable and Complementary Adsorbents of Coal-Based and Bio-Based Humic Acids: High Efficient Adsorption and Immobilization Remediation for Pb(II) Contaminated Water and Soil. *Chemosphere*, **318**; 137963

Zhou, Y., Y. Zhang, P. Li, and G. Li (2014). Comparative Study on the Adsorption Interactions of Humic Acid onto Natural Magnetite, Hematite and Quartz: Effect of Initial HA Concentration. *Powder Technology*, **251**; 1–8

Zong, E., R. Fan, H. Hua, J. Yang, S. Jiang, J. Dai, and X. Liu (2022). A Magnetically Recyclable Lignin-Based Bio-Adsorbent for Efficient Removal of Congo Red from Aqueous Solution. *International Journal of Biological Macromolecules*, **226**; 443–453

